ELSEVIER

Journal of Alloys and Compounds 303–304 (2000) 104–111

Journal of ALLOYS AND COMPOUNDS

www.elsevier.com/locate/jallcom

Interaction of trivalent lanthanide cations with phosphoryl derivatives, amide, anisole, pyridine and triazine ligands: a quantum mechanics study

M. Baaden, F. Berny, C. Boehme, N. Muzet, R. Schurhammer, G. Wipff*

Laboratoire MSM, Institut de Chimie, Université Louis Pasteur, UMR CNRS 7551, 4, Rue B. Pascal, 67000 Strasbourg, France

Abstract

We report ab initio quantum mechanical calculations on charged $\mathbf{L}M^{3+}$ and neutral $\mathbf{L}MCl_3$ complexes formed by lanthanide M^{3+} cations (M=La, Eu, Yb) and model ligands **L**, where **L** are phosphorous derivatives R_3PO (R=alkyl/*O*-alkyl/phenyl), R_3PS and $R_2PS_2^-$ (R=alkyl/phenyl), and amide, pyridine, triazine and anisole ligands. Among all neutral ligands studied, Ph_3PO is intrinsically clearly the best. However, the comparison of $\mathbf{L}M^{3+}$ to $\mathbf{L}MCl_3$ complexes demonstrates that the concept of 'ligand basicity' is not sufficient to compare the efficiency of cation coordination. Counterions play an important role in the structures of the complexes and for the consequences of substitution in the ligand. For instance, in the absence of competing interactions, phenyl substituted R_3PS or $R_2PS_2^-$ ligands interact better than alkyl substituted ones, but the order is reversed in the presence of counterions. Counterions also amplify the alkyl vs. *O*-alkyl substituent effect in R_3PO complexes. Bidentate anions or more bulky anions are expected to amplify the effects observed with chloride anions. Thus, multiple interactions between counterions and the other species in the first coordination sphere markedly contribute to the 'effectiveness' and stereochemistry of ligand–cation interactions.

Keywords: Lanthanides; Ionophores; Liquid–liquid ion extraction

1. Introduction

The search for complexant molecules which specifically bind lanthanides and actinides and separate them from other cations may be guided by an assessment of the intrinsic energetic and stereochemical features of the cation–ligand interactions 'in the gas phase', i.e. in the absence of any other competing factor [1–3]. Gas phase data on simple systems contribute to a better understanding, by comparison, of what happens in solution with more complex ones [4,5]. In the case of trivalent lanthanide or actinide ions, such data are not available. Quantum mechanical (QM) computations offer an alternative source of valuable information on structural, electronic and energy features of non-covalent interactions [6]. In this paper, we report on recent QM ab initio results on the interaction between M^{3+} lanthanide cations (M=La vs. Eu vs. Yb) and important types of ligands **L**: phosphorous derivatives of R_3PO (R=alkyl/*O*-alkyl/phenyl), R_3PS, $R_2PS_2^-$ (R=alkyl/phenyl) type, and amide, pyridine, triazine and anisole ligands (Figs. 1–3). We first consider the charged 1:1 $\mathbf{L}M^{3+}$ complexes and calculate the corresponding interaction energies ΔE between **L** and M^{3+} in the absence of other competing interactions. In addition, the effect of neutralizing counterions is investigated for $\mathbf{L}MCl_3$ complexes, which are closer to those expected in condensed phases, both in terms of metal cation effective charge and coordination number. Indeed, in liquid–liquid extraction experiments, the cation is neutralized by accompanying counterions. In solid state structures, most of the lanthanide and actinide cations are also coordinated by neutralizing counterions. Our aim is to compare the ΔE values of a given cation and these ligands **L**. The amide and pyridine complexes are described in Ref. [7]. Some results for **L**=Me_3PO and Ph_3PO have been reported by Troxler et al. [8] but they have been reoptimized in order to allow for a consistent comparison with the other ligands. A detailed analysis of R_3PS, $R_2PS_2^-$ and $(MeO)_3PO$ complexes can be found in Refs. [9–11].

2. Methods

The QM ab initio calculations were performed at the HF level using the Gaussian-94 [14] and Gaussian-98 pack-

*Corresponding author.

E-mail address: wipff@chimie.u-strasbg.fr (G. Wipff)

0925-8388/00/$ – see front matter
PII: S0925-8388(00)00657-5

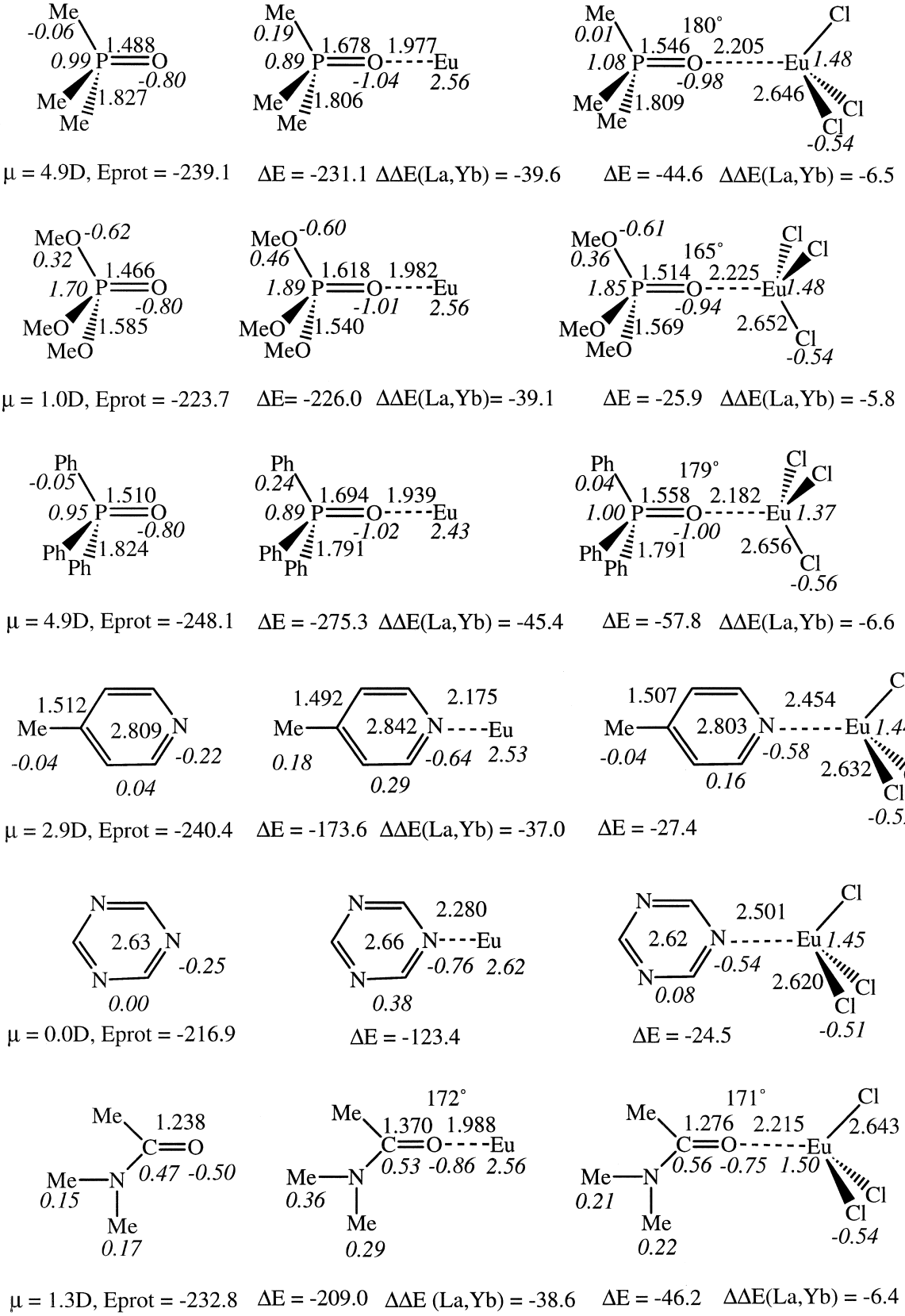

Fig. 1. Optimized distances (Å) and angles (°) in the free ligands **L** (left), the $\mathbf{L}M^{3+}$ (center) and $\mathbf{L}MCl_3$ (right) complexes. Mulliken charges (in italics) on selected fragments or atoms. ΔE is the interaction energy (kcal mol^{-1}) between **L** and Eu^{3+} (in $\mathbf{L}Eu^{3+}$ complexes) or between **L** and $EuCl_3$ (in $\mathbf{L}EuCl_3$ complexes). $\Delta\Delta E$(La,Yb) is the difference in the interaction energies calculated in the corresponding Yb^{3+} and La^{3+} complexes. (**L**=Me_3PO; $(MeO)_3PO$; Ph_3PO; Me–pyridine; 1,3,5-triazine; *N*,*N*-dimethylacetamide.)

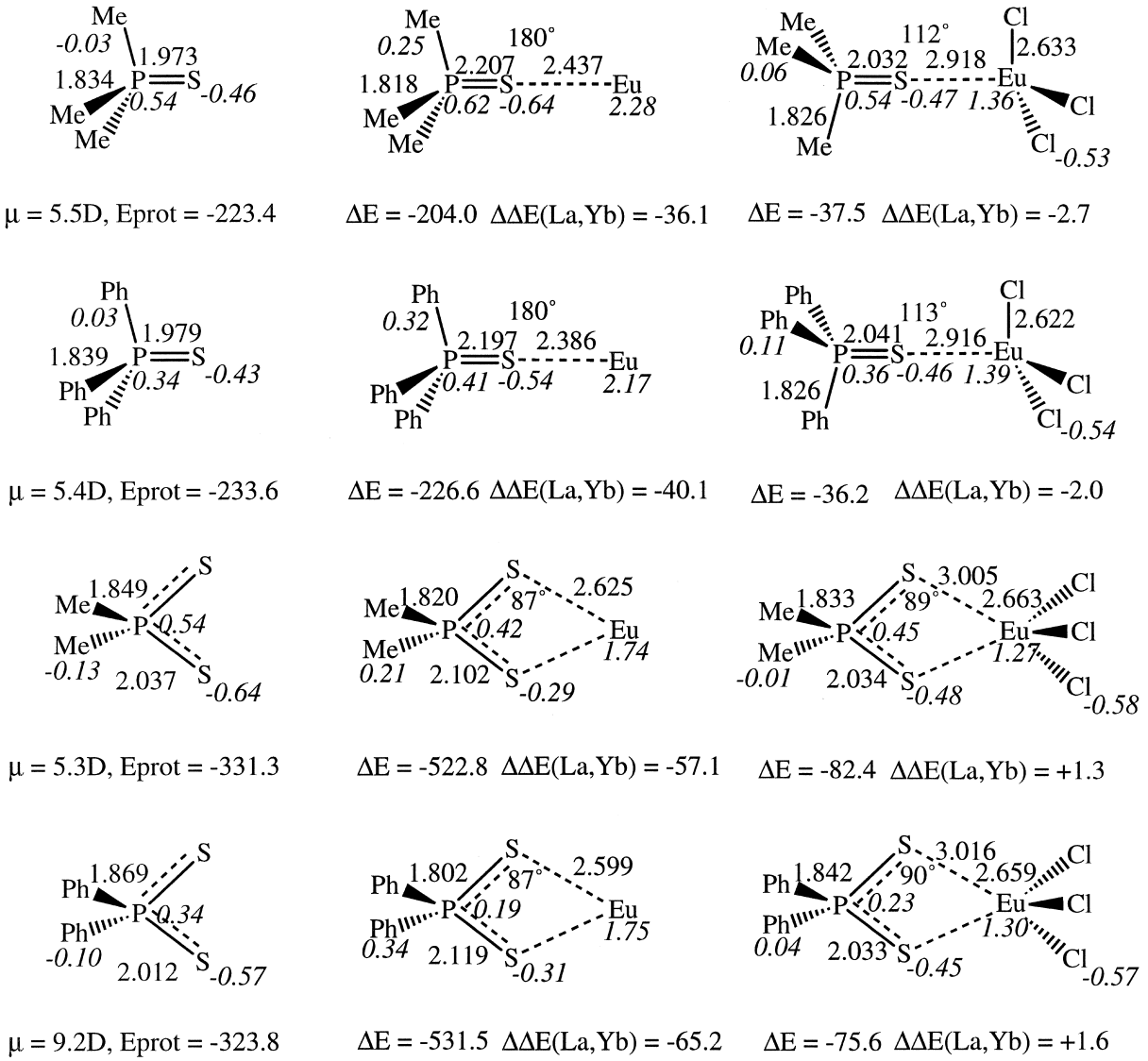

Fig. 2. See definitions in Fig. 1. **L**=Me_3PS; Ph_3PS; $Me_2PS_2^-$; $Ph_2PS_2^-$.

ages [15]. The $46+4f^n$ core electrons of the lanthanide cations were described by the quasi-relativistic effective core potential (ECP) of Dolg et al. [16,17] and the valence electrons by a (7s,6p,5d)/[5s,4p,3d] Gaussian basis set supplemented by one f polarization function of exponent 0.591 [18]. The H, C, N, O, S and P atoms were described by the standard Dunning–Hay double-ζ basis set [19] including one 3d polarization function on the P atom (of exponent $\zeta_{3d}=0.37$) and on the S atom ($\zeta_{3d}=0.532$) (referred to hereafter as 'DZ' basis set). In additional calculations, polarization functions on the atoms of **L** and on Cl atoms were also included (exponents being $\zeta_{3dC}=0.75$, $\zeta_{3dO}=0.85$, $\zeta_{3dN}=0.80$, $\zeta_{2pH}=0.80$, $\zeta_{3dCl}=0.60$), leading to the DZ* basis set.

The R_3PS and $R_2PS_2^-$ ligands and the corresponding complexes were fully optimized using analytical gradients and the DZ* basis set. The other ligands and their protonated forms $\mathbf{L}H^+$ were similarly optimized with the DZ* basis set. Their $\mathbf{L}M^{3+}$ and $\mathbf{L}MCl_3$ complexes were optimized with the DZ basis set as described in Refs. [9,10] and the corresponding interaction energies ΔE, Mulliken charges and dipole moments were recalculated with the DZ* basis set.

The interaction energies ΔE of the ligands were calculated as $\Delta E=E(\mathbf{L}M^{3+})-E(\mathbf{L})-E(M^{3+})$ in the $\mathbf{L}M^{3+}$ complexes, and as $\Delta E=E(\mathbf{L}MCl_3)-E(\mathbf{L})-E(MCl_3)$ in the $\mathbf{L}MCl_3$ complexes, using all optimized corresponding geometries. The basis set superposition error ('BSSE') was estimated in typical cases using the counterpoise method [20]. As the BSSE was small and nearly constant (from

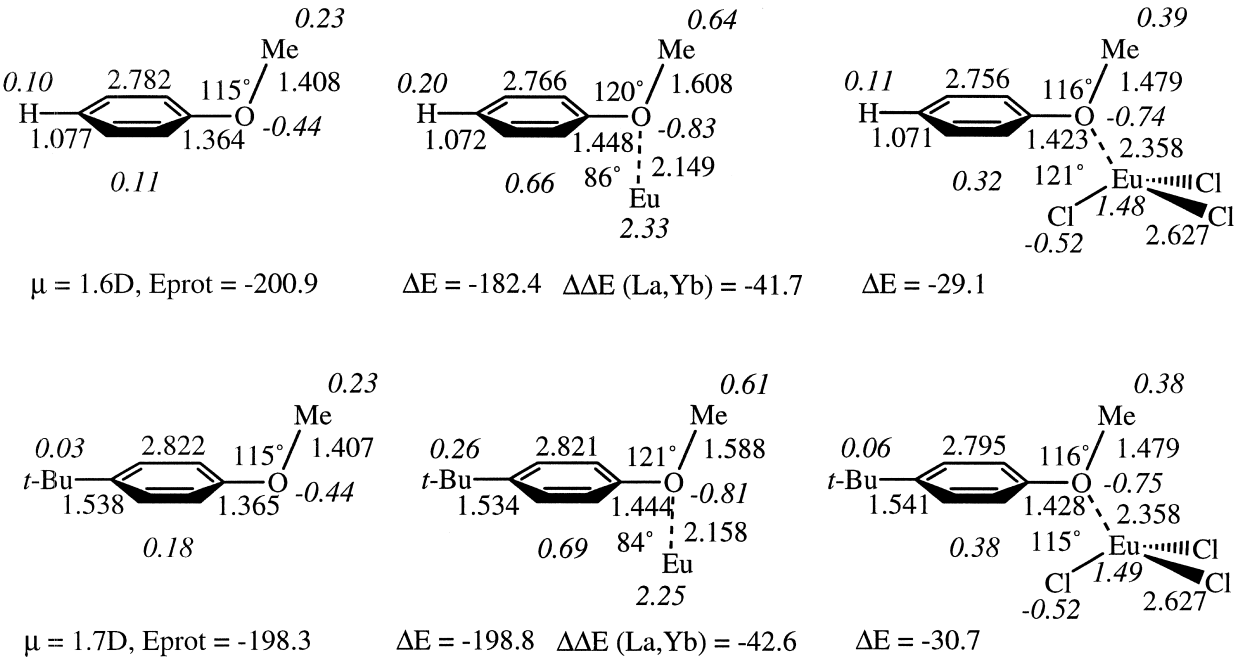

Fig. 3. See definitions in Fig. 1. **L**=Anisole; *t*-Bu-anisole.

−2 to −4 kcal mol^{-1}), we report the uncorrected ΔE values for simplicity.

3. Results and discussion

The most important energy, structural (distances and angles) and electronic (atomic charges) results are summarized in Figs. 1–3. For any given ligand **L**, ΔE in the $\mathbf{L}M^{3+}$ complexes increases with the cation hardness ($La^{3+}<Eu^{3+}<Yb^{3+}$). This is why, for simplicity, we primarily discuss complexes with Eu^{3+}, which is the cation of intermediate size, and report the corresponding ΔE, as well as the $\Delta\Delta E$(La,Yb) energy difference between the La^{3+} and Yb^{3+} complexes, which measures the 'cation selectivity' of a given ligand **L**. A graphical representation of ΔE values and protonation energies E_{prot} of **L** is given in Fig. 5.

Depending on the nature of the dominant electrostatic interactions calculated, the ΔE values fall in three categories. The strongest interactions are of charge–charge type ($R_2PS_2^- - M^{3+}$; ΔE is about 530 kcal mol^{-1}). They are followed by charge–dipole interactions in $\mathbf{L}M^{3+}$ complexes with the neutral ligands (from 123 to 280 kcal mol^{-1}) and to a lesser extent in the $R_2PS_2^- - MCl_3$ complexes with the charged ligands (about 80 kcal mol^{-1}), and finally by dipole–dipole interactions in $\mathbf{L}MCl_3$ complexes with neutral ligands (from 25 to 46 kcal mol^{-1}). Among the $\mathbf{L}M^{3+}$ complexes with neutral ligands, ΔE decreases in the order $Ph_3PO>Me_3PO>Ph_3PS$, $(MeO)_3PO>$amide$>Me_3PS>t$-Bu-anisole$>$anisole$>$pyridine$>$triazine in the $\mathbf{L}M^{3+}$ complexes. The sequence is somewhat different in the corresponding $\mathbf{L}MCl_3$ complexes ($Ph_3PO>$amide, $Me_3PO>Me_3PS$, $Ph_3PS>t$-Bu-anisole$>$anisole$>$pyridine$>(MeO)_3PO>$triazine), showing that *counterions may modulate or reverse the order of interaction energies*. We notice that differences in ΔE values in the $\mathbf{L}MCl_3$ series are small, and may be changed by substituents, as well as by subtle geometry modifications.

Although the definition of atomic charges is somewhat arbitrary and numerical values are basis set dependent, one observes (Figs. 1–3) important electron transfer to the cation. Its positive charge is about 2.3*e* to 2.6*e* in $\mathbf{L}Eu^{3+}$ (**L**=R_3PO, amide, anisole, pyridine, triazine), 2.2*e* in R_3PSEu^{3+}, 1.7*e* in $R_2PS_2Eu^{2+}$, and 1.3*e* to 1.5*e* in the neutral $\mathbf{L}EuCl_3$ complexes. There is, however, no simple relation between the charge transfer to the cation and the corresponding interaction energies ΔE, nor between the permanent dipole moment of the free ligands **L** and the ΔE values (Figs. 1–3).

In the following, we first discuss the interaction energies ΔE and structural features of the phosphoryl R_3PO complexes with Eu^{3+} and $EuCl_3$. We compare how the different substituents R influence the ΔE values in the absence and in the presence of counterions. We also address the cation discrimination of the ligands in terms of the differences in interaction energies $\Delta\Delta E$(La,Yb) between the largest and the smallest cation studied. The final part covers how the thiophosphoryl (R_3PS), dithiophosphi-

nate ($R_2PS_2^-$), amide, anisole and pyridine complexes differ from the phosphoryl complexes from an energetic and from a structural point of view. The calculated ΔE values and protonation energies of the ligands are shown in Figs. 1–3.

3.1. Complexes with phosphoryl $R_3P{=}O$ ligands (R= alkyl/phenyl/O-alkyl)

The coordination of the phosphoryl ligands to a 'naked' Eu^{3+} cation leads to very high dipole–charge interaction energies of more than 200 kcal mol^{-1}. In the process of coordination the ligand is strongly polarized (see Fig. 4) by the neighboring charge, as can be seen from the lengthening of the P–O bond. In the free Ph_3PO ligand, for example, the P–O bond length is 1.510 Å, corresponding to a partial double bond. In the Ph_3POEu^{3+} complex, electron density is moved from the P–O bond to the oxygen atom, resulting in a P–O single bond with a length of 1.694 Å. This effect can also be seen in the oxygen charge, which becomes more negative. Such an increase of negative charge on the connecting atom from the free to the complexed ligand is found for all complexes with neutral ligands, showing that the electron transfer to the metal stems from more remote atoms.

The pronounced *ligand polarization* is the key to understanding the influence of the substituents R on the ΔE values. Phenyl is the largest and most polarizable substituent. Therefore, Ph_3PO yields the strongest ligand–metal interaction, nearly 50 kcal mol^{-1} more than the next best ligand, Me_3PO. Substituting methyl for the more electronegative methoxy group gives the expected lowering of ΔE, but the effect is surprisingly small (only 5 kcal mol^{-1}). The change in the electronegativity of R from the methoxy to the methyl group has a smaller effect than the change of polarizability from methyl to phenyl.

The interaction energies of the discussed ligands are strongly dependent on the cation size. The $\Delta\Delta E$(La,Yb) value is about 40 kcal mol^{-1} for all R_3PO ligands. The $\Delta\Delta E$ values follow the trend of the ΔE values, i.e. the largest cation discrimination is observed with phenyl as substituent. This substituent effect is small, however. The difference between phenyl and methoxy groups in this respect is only about 6 kcal mol^{-1}.

The addition of counterions to the metal cation leads to a marked drop in ΔE, by a factor of 5.2 with Me_3PO, of 4.8 with Ph_3PO and of 8.7 with $(MeO)_3PO$. Upon addition of counterions the hard dipole–charge interaction is substituted by a weaker and softer dipole–dipole interaction. This shows in a less pronounced polarization of the ligand which in turn leads to a less pronounced change of its

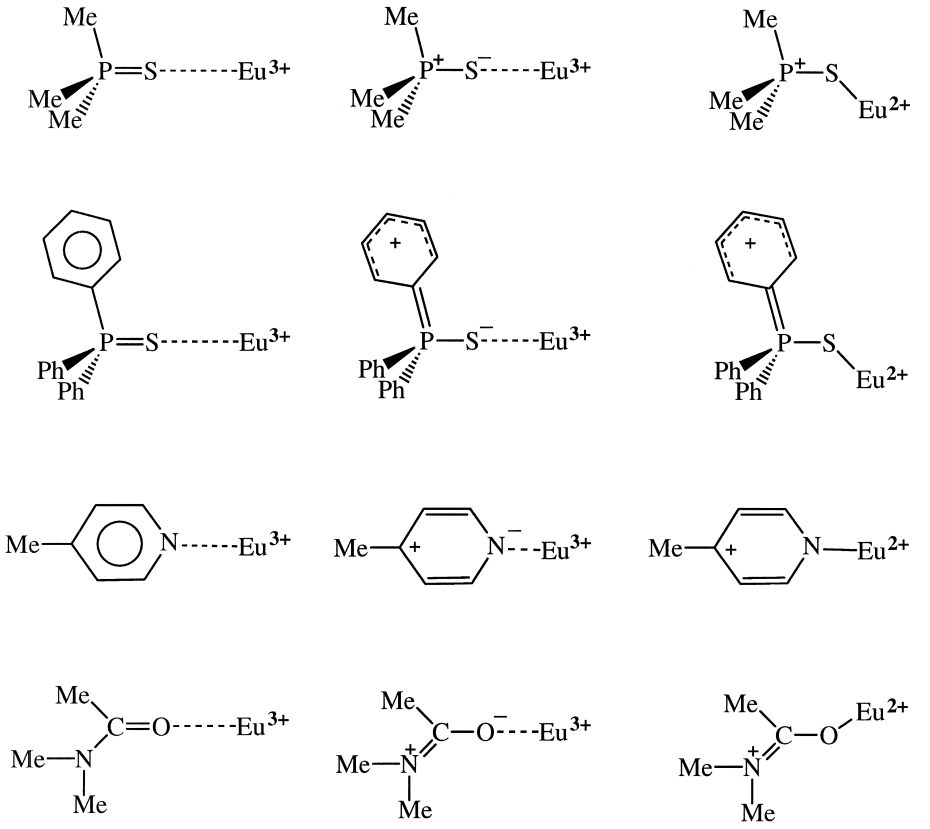

Fig. 4. Schematic representation of $\mathbf{L}M^{3+}$ complexes, which highlight the interactions between the cation and the unperturbed ligand (left), the polarization of **L** by the cation (center) and the covalent character of the **L**igand–Metal bond (right).

structure. For example, the P–O bond elongation from the free to the complexed ligand is only 0.05 Å in $Ph_3POEuCl_3$ compared to 0.18 Å in Ph_3POEu^{3+}. The connecting oxygen atom is also more negatively charged than in the free ligand. For Ph_3PO, the oxygen charge changes by −0.22 in the $\mathbf{L}M^{3+}$ complex and by −0.20 in the $\mathbf{L}MCl_3$ complex. The occurrence of covalent effects can be seen from the slight bending about the oxygen atom in some neutral complexes, which can be explained by bonding orbital directionality. Changing the type of ligand–metal interactions also reduces the influence of the substituents R on ΔE values. In fact, the phenyl substituted ligand Ph_3PO still yields a higher interaction energy with MCl_3 than the alkyl-substituted Me_3PO, but the difference drops to about 13 kcal mol^{-1}. The high polarizability of the phenyl ligand is less important here. Furthermore, ΔE is negatively influenced by phenyl–chloride repulsions and the higher electronegativity of the phenyl compared to the methyl carbon. The effects of ligand–counterion repulsions and ligand electronegativity also show in the huge difference in ΔE (about 20 kcal mol^{-1}) between Me_3POMCl_3 and $(MeO)_3POMCl_3$ complexes. Along with the decrease of ΔE in the neutral complexes the cation discriminating capabilities of the ligands also decrease, with $\Delta\Delta E$(La,Yb) dropping from 40 kcal mol^{-1} in the charged $\mathbf{L}M^{3+}$ to about 6 kcal mol^{-1} in the neutral $\mathbf{L}MCl_3$ complexes. Substituent effects on cation discrimination are negligible here.

3.2. Complexes with neutral ligands: thiophosphoryl R_3PS, amide, pyridine, 1,3,5-triazine and anisole

In the $\mathbf{L}Eu^{3+}$ complexes with neutral monodentate ligands, none yields a ΔE interaction as strong as the phosphoryl ligands. The amide and the best studied thiophosphoryl (Ph_3PS) ligand yield ΔE values of 209 and 225 kcal mol^{-1}, respectively, compared to about 280 kcal mol^{-1} in Ph_3POEu^{3+}. The unsubstituted anisole interacts better than the pyridine (182 and 174 kcal mol^{-1}, respectively), while its *t*-butyl derivative interacts only 10 kcal mol^{-1} less than the amide, revealing a marked *para* substituent effect (of about 16 kcal mol^{-1}). The triazine (123 kcal mol^{-1}) ligand yields the lowest ΔE, which is 51 kcal mol^{-1} less than with pyridine, as a result of the zero dipole moment of triazine, and of the higher electronegativity and lower polarizability of the two additional nitrogen atoms in its ring system.

The phenyl vs. alkyl substituent effects on ΔE values follow the same order for the thiophosphoryl and amide complexes as observed for the phosphoryl ones. In the $\mathbf{L}Eu^{3+}$ complexes, Ph_3PS yields a ΔE about 20 kcal mol^{-1} higher than Me_3PS and the HPh-amide ligand gives a ΔE about 8 kcal mol^{-1} higher than the HMe-amide [9]. This is less than the difference between the Ph_3PO and Me_3PO complexes (about 50 kcal mol^{-1}).

The addition of counterions to the $\mathbf{L}M^{3+}$ complexes leads to a drop of the ΔE values, and a lengthening of the metal–ligand bond distances. In addition, for the R_3PSMCl_3 complexes, Fig. 2 reveals two important effects. First, the order of alkyl vs. phenyl substituents is reversed, i.e. ΔE is smaller (by about 1 kcal mol^{-1}) in the $Ph_3PSEuCl_3$ complex than in the $Me_3PSEuCl_3$ complex. The second feature concerns the marked soft and covalent character of the metal–sulfur bond, which leads to a pronounced bending at the sulfur atom (about 112°; see Fig. 2). This bending makes sulfur-based organophosphorous compounds excellent candidates for bidentate ligands in which binding coordination has to be bent. As bonding in actinide complexes is generally more covalent than in lanthanide ones, discrimination of actinides is expected to be enhanced with thiophosphoryl bidentate ligands.

3.3. Complexes with negatively charged dithiophosphinate ($R_2PS_2^-$) ligands

With the naked Eu^{3+} cation, $R_2PS_2^-$ ligands yield interaction energies of more than 520 kcal mol^{-1}, the latter being higher with R=phenyl than with R=methyl. The difference, however, is smaller (about 9 kcal mol^{-1}) than with the neutral ligands, as a charge–charge interaction is less influenced by the choice of substituents and polarization effects are relatively less important. The addition of three counterions to the metal leads to negatively charged complexes $R_2PS_2EuCl_3^-$. The corresponding ΔE values (about 80 kcal mol^{-1}) are about 40 kcal mol^{-1} higher than for the R_3PS and R_3PO complexes, which represents the gain of charged vs. neutral ligands and of bidentate vs. monodentate bonding.

It is interesting that in the dithiophosphinate complexes the charge on the connecting (sulfur) atoms becomes more positive upon complexation, the effect being opposite to that found for all neutral ligands. Furthermore, the positive charge on the metal atom decreases more than with the neutral ligands, especially in the complexes without counterions. This is related to an increased charge-transfer to the metal, which is facilitated by the negative charge on **L** and better orbital overlap in the bent structure. As with the R_3PS complexes, *the order of alkyl vs. phenyl substituent effects is reversed when counterions are added to the system*. The cation discrimination behavior in the $R_2PS_2MCl_3^-$ complexes is also very interesting: *the large La cation is bonded stronger than the small Yb* (by 1–2 kcal mol^{-1}). Whether this is a result of ligand–ligand repulsion or a more subtle ligand interaction effect is a matter of ongoing research.

4. Conclusion

Quantum mechanical studies on the interactions between lanthanide cations and typical ligand molecules provide

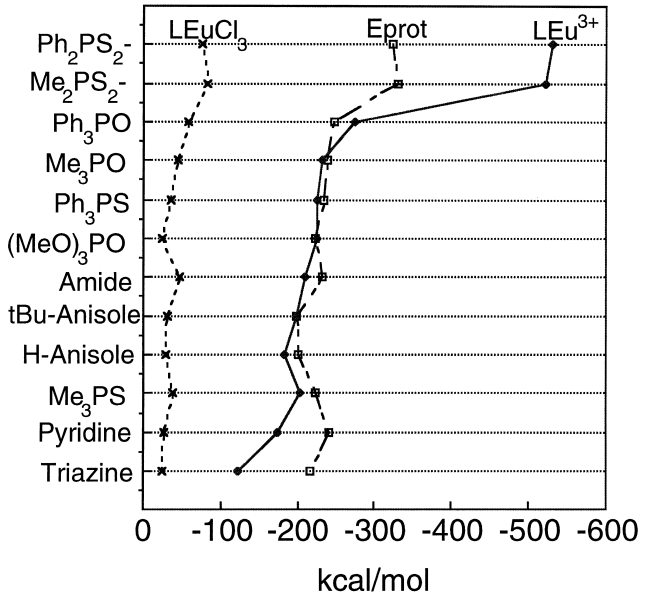

Fig. 5. Graphical representation of calculated interaction energies ΔE in the $\mathbf{L}Eu^{3+}$ and $\mathbf{L}EuCl_3$ systems, and protonation energies (E_{prot}) of **L** (kcal mol^{-1}).

important insights into their intrinsic structural and energy features. A graphical representation of the results is given in Fig. 5.

Intrinsically, for any ligand (i.e. without counterions), the interaction energies ΔE values increase as expected with the cation hardness (from La^{3+} to Yb^{3+}). Among the neutral ligands studied here, phosphoryl ligands give the largest interaction energies ΔE. Following are the amide, thiophosphoryl, anisole and pyridine ligands. The triazine ligand, which mimics the central moiety of TPTZ [21] is markedly weaker bound than the others. The negatively charged bidentate dithiophosphinate ligands which model CYANEX 301 molecules [22–24], yield higher ΔE values than the neutral ligands. We notice however that the differences in ΔE values for $\mathbf{L}M^{3+}$ complexes with neutral ligands such as Ph_3PS, Me_3PO, $(MeO)_3PO$, amide and anisole are smaller than the changes in ΔE values related to substituent effects in some ligands (about 50 kcal mol^{-1} for Ph vs. Me substituents in R_3POM^{3+} complexes, and about 90 kcal mol^{-1} in NMe_2 vs. NO_2 *para*-substituted pyridine complexes [9]). Replacement of Me by larger and more polarizable Alkyl groups may therefore also modulate the sequence of binding affinities. The comparison of *t*-Bu-anisole and amide ligands indicates that cation encapsulation at the lower rim of calixarene derivatives (e.g. of amide, ester or phosphoryl type) [25–28] results from a significant participation (from 40 to 50%) of the calixarene moiety, including the stabilizing role of 'upper rim' remote substituents.

Regarding the phenyl vs. alkyl substituent effects in the R_3PO, R_3PS or $R_2PS_2^-$ ligands, the more polarizable aryl substituents are intrinsically better than alkyl ones in the absence of other competing interactions. However, in the presence of counterions, this order is reversed with R_3PS and $R_2PS_2^-$ ligands, the alkyl substituted ligands being preferred. Concerning the alkyl vs. *O*-alkyl substituent effect in R_3PO complexes, we find that counterions *amplify* the preference of alkyl substituted ligands [12,13]. Thus, our study shows clearly that *counterions have a very strong influence on the ligand–metal interactions*, which means that any data regarding the ligand alone, like intrinsic ligand basicity, is insufficient to assess its interactions in condensed phases where the first coordination sphere is saturated. The counterion effects are expected to increase with more bulky or bidentate anions (nitrate, phosphate, carboxylate, etc.). Furthermore, the stoichiometry of the complexes, as well as the coordination of other species (e.g. solvent molecules) to the metal are additional environmental effects that may modify ligand–metal interactions. Thus, care should be taken in the analysis of such interactions in condensed phases solely in terms of the characteristics of the partners (donor–acceptor, acid–base HSAB [29–32], etc.). Ligand–metal interactions depend on medium effects as well as on other interactions in the first coordination sphere ('steric effects'). Intrinsic basicities, as determined by the gas phase protonation energies (see E_{prot} values in Figs. 1–3, and plot in Fig. 5) may not properly reflect trends in condensed phases.

These counterion and environment effects may play an important role in the design of ionophores. Marked modulation of stabilities and selectivities may be expected when, for topological reasons (preorganisation, cooperativity effects, . . .), the binding sites of the ligand wrap around the metal sufficiently to prevent direct coordination of counterions to the metal.

Ion complexation in solution is a much more complicated process, compared to the gas phase. Its thermodynamics depends on enthalpic and entropic contributions involving large numbers of configurations of uncomplexed and complexed states. Ion–ligand interactions compete with large changes in solvation properties. Thus, cumulative dynamic effects arising from multiple ligand, solvent and counterion coordination to the cation need to be incorporated in the simulated system. This can be achieved in principle by combining a QM representation of the 'core' of the system (e.g. the cation's first coordination sphere) with simpler models (e.g. of force field type) for the remaining system [33,34], but remains a challenge for simulation methods.

Acknowledgements

The authors are grateful to the EU for support (Marie Curie grant for CB, Contract Nos. F14W-CT98-5003 and F14WCT0022), and to the IDRIS and Université Louis Pasteur for allocation of computer resources. MB, FB, NM

and RS are grateful to the French Ministry of Research for a grant.

References

[1] J.M. Lehn, Struct. Bonding 161 (1973) 1–69.
[2] J.-C. Bünzli, D. Wessner, Coord. Chem. Rev. 60 (1984) 191–253.
[3] V. Alexander, Chem. Rev. 95 (1995) 273–342.
[4] I.-H. Chu, H. Zhang, D. Dearden, J. Am. Chem. Soc. 115 (1993) 5736–5744.
[5] P. Kebarle, Ann. Rev. Phys. Chem. 28 (1977) 445–476.
[6] P. Kollman, J. Am. Chem. Soc. 99 (1977) 4875.
[7] K. Morokuma, Acc. Chem. Res. 10 (1977) 294.
[8] M. Badertscher, M. Welti, P. Portmann, E. Pretsch, Topics Curr. Chem. 136 (1986) 17, and references cited.
[9] F. Berny, N. Muzet, L. Troxler, A. Dedieu, G. Wipff, Inorg. Chem. 38 (1999) 1244–1252.
[10] L. Troxler, A. Dedieu, F. Hutschka, G. Wipff, J. Mol. Struct. (THEOCHEM) 431 (1998) 151–163.
[11] C. Boehme, G. Wipff, J. Phys. Chem. A 103 (1999) 6023–6029.
[12] C. Boehme, G. Wipff, Inorg. Chem. 38 (1999) 5734–5741.
[13] R. Schurhammer, V. Erhart, L. Troxler, G. Wipff, J. Chem. Soc., Perkin Trans. (1999) 2515–2534.
[14] M.J. Frisch, G.W. Trucks, H.B. Schlegel, P.M.W. Gill, B.G. Johnson, M.A. Robb, J.R. Cheeseman, T. Keith, G.A. Petersson, J.A. Montgomery, K. Raghavachari, M.A. Al-Laham, V.G. Zakrzewski, J.V. Ortiz, J.B. Foresman, C.Y. Peng, P.Y. Ayala, W. Chen, M.W. Wong, J.L. Andres, E.S. Reploge, R. Gomperts, F.D.J. Martin, J.S. Binkley, D.J. Defrees, J. Baker, J.P. Stewart, M. Head-Gordon, C. Gonzales, J.A. Pople, Gaussian 94, Rev. B.2, Gaussian, Pittsburgh, PA, 1995.
[15] M.J. Frisch, G.W. Trucks, H.B. Schlegel, G.E. Scuseria, M.A. Robb, J.R. Cheeseman, V.G. Zakrzewski, J.A. Montgomery Jr., R.E. Stratmann, J.C. Burant, S. Dapprich, J.M. Millam, A.D. Daniels, K.N. Kudin, M.C. Strain, O. Farkas, J. Tomasi, V. Barone, M. Cossi, R. Cammi, B. Mennucci, C. Pomelli, C. Adamo, S. Clifford, J. Ochterski, G.A. Petersson, P.Y. Ayala, Q. Cui, K. Morokuma, D.K. Malick, A.D. Rabuck, K. Raghavachari, J.B. Foresman, J. Cioslowski, J.V. Ortiz, B.B. Stefanov, G. Liu, A. Liashenko, P. Piskorz, I. Komaromi, R. Gomperts, R.L. Martin, D.J. Fox, T. Keith, M.A. Al-Laham, C.Y. Peng, A. Nanayakkara, C. Gonzalez, M. Challacombe, P.M.W. Gill, B. Johnson, W. Chen, M.W. Wong, J.L. Andres, C. Gonzalez, M. Head-Gordon, E.S. Replogle, J.A. Pople, Gaussian 98, Rev. A.5, Gaussian, Pittsburgh, PA, 1998.
[16] M. Dolg, H. Stoll, A. Savin, H. Preuss, Theoret. Chim. Acta 75 (1989) 173.
[17] M. Dolg, H. Stoll, A. Savin, H. Preuss, Theoret. Chim. Acta 85 (1993) 441.
[18] A.W. Ehlers, M. Böhme, S. Dapprich, A. Gobbi, A. Höllwarth, V. Jonas, K.F. Köhler, R. Stegmann, A. Veldkamp, G. Frenking, Chem. Phys. Lett. 208 (1993) 111.
[19] T.H. Dunning, P.J. Hay, in: Modern Theoretical Chemistry, Plenum, New York, 1976, pp. 1–28.
[20] S.F. Boys, F. Bernardi, Mol. Phys. 19 (1970) 553–566.
[21] G.Y.S. Chan, M.G.B. Drew, M.J. Hudson, N.S. Isaacs, P. Byers, C. Madic, Polyhedron 15 (1996) 3385–3398.
[22] C. Hill, C. Madic, P. Baron, M. Ozawa, Y. Tanaka, J. Alloys Comp. 271–273 (1998) 159–162.
[23] Y. Zhu, Radiochimica Acta 68 (1995) 95–98.
[24] G. Modolo, R. Odoj, Solv. Extract. Ion Exch. 17 (1999) 33–53.
[25] A. Arduini, E. Ghidini, A. Pochini, R. Ungaro, G.D. Andreetti, G. Calestani, F. Ugozzoli, J. Inclus. Phenom. 6 (1988) 119–134.
[26] M.R. Yaftian, M. Burgard, D. Matt, C.B. Dieleman, F. Rastegar, Solv. Extract. Ion Exch. 15 (1997) 975–989.
[27] J.F. Malone, D.J. Marrs, A. McKervey, P. O'Hagan, N. Thompson, A. Walker, F. Arnaud-Neu, O. Mauprivez, M.-J. Schwing, J.-F. Dozol, H. Rouquette, N. Simon, J. Chem. Soc. Chem. Commun. (1995) 2151–2153.
[28] F. Arnaud-Neu, J.K. Browne, D. Byrne, D.J. Marrs, M.A. McKervey, P. O'Hagan, M.-J. Schwing-Weill, A. Walker, Chem. Eur. J. 5 (1999) 175–186.
[29] R.G. Pearson, Coord. Chem. Rev. 100 (1990) 403–425.
[30] Y. Marcus, Ion Solvation, Wiley, Chichester, 1985.
[31] A.E. Martell, R.D. Hancock, Metal Complexes in Aqueous Solutions, Plenum Press, New York, 1996.
[32] R.D. Hancock, A.E. Martell, Chem. Rev. 89 (1989) 1875–1914.
[33] M.A. Thompson, E.D. Glendening, D. Feller, J. Am. Chem. Soc. 116 (1994) 10465–10476.
[34] J. Gao, Acc. Chem. Res. 29 (1996) 298–305.